# LANGMUIR

pubs.acs.org/Langmuir Article

# Imidazolinium N-Heterocyclic Carbene Ligands for Enhanced Stability on Gold Surfaces

Lindy M. Sherman, Shelby L. Strausser, Rowan K. Borsari, David M. Jenkins,\* and Jon P. Camden\*



Cite This: Langmuir 2021, 37, 5864-5871



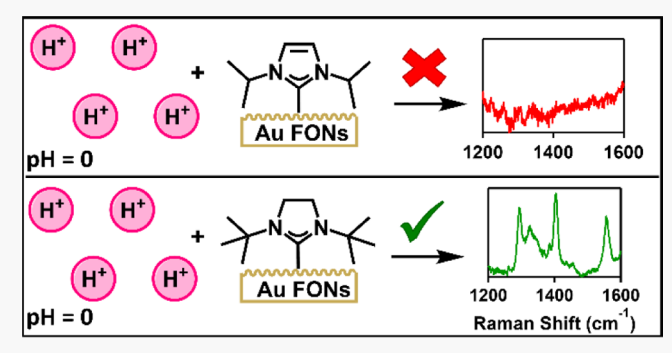
ACCESS

Metrics & More

Article Recommendations

Supporting Information

ABSTRACT: N-heterocyclic carbenes (NHCs) have emerged as versatile and robust ligands for noble metal surface modifications due to their ability to form compact, self-assembled monolayers. Despite a growing body of research, previous NHC surface modification schemes have employed just two structural motifs: the benzimidazolium NHC and the imidazolium NHC. However, different NHC moieties, including saturated NHCs, are often more effective in homogenous catalysis chemistry than these aforementioned motifs and may impart numerous advantages to NHC surfaces, such as increased stability and access to chiral groups. This work explores the preparation and stability of NHC-coated gold surfaces using imidazolium and imidazolinium NHC ligands.



X-ray photoelectron spectroscopy and surface-enhanced Raman spectroscopy demonstrate the attachment of NHC ligands to the gold surface and show enhanced stability of imidazolinium compared to the traditional imidazolium under harsh acidic conditions.

### 1. INTRODUCTION

Controlling the surface environment on metal substrates via ligand chemistry is essential for applications ranging from catalysis to sensing and therapeutics. 1-6 Despite the welldocumented challenges associated with thiol ligands, such as oxidation and degradation under ambient conditions, 7-11 they remain the most common molecule class for functionalizing noble metal surfaces due to their high affinity for gold and silver. For example, recent reports have employed thiol-based ligands to develop patterned molecular films for site-specific immobilization of biomolecules, 12,13 to investigate host—guest complexation for surface detection of polycyclic aromatic hydrocarbons, 14 and to tether aptamers on implantable electrochemical devices for in vivo diagnostics. 15,16 In 2014, Crudden and co-workers<sup>17</sup> reported that N-heterocyclic carbene (NHC) ligands form stable, well-ordered, and selfassembled monolayers on crystalline gold that can, in many situations, exceed the performance of thiols. Since their initial work, multiple research groups have explored the capabilities of NHC-coated surfaces toward a variety of applications. 18-24

Despite the increasing popularity of NHCs for noble metal surface modification, previous investigations of NHCs on gold have focused almost exclusively on the traditional NHC motifs: imidazolium (Figure 1A) and benzimidazolium (Figure 1B). These two designs are widely employed because their precursor salts are synthesized *via* straightforward protocols with commercially available imidazole or benzimidazole as starting materials. <sup>17,25</sup> The NHC–CO<sub>2</sub> adducts employed for surface deposition can then be synthesized *via* a deprotonation reaction in a strong base. <sup>19,26</sup> The presence of the NHC ligand

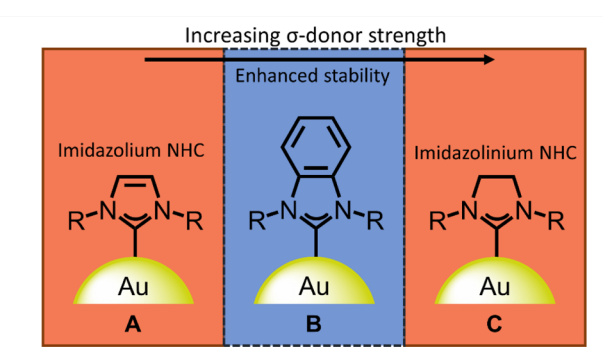


**Figure 1.** Comparison of traditional (A,B) and less-explored (C) NHC structures on gold surfaces. Imidazolium (A) and imidazolinium (C) are the focus of this work.

on the substrate surface has been monitored using a variety of techniques, particularly scanning tunneling microscopy (STM),<sup>27</sup> atomic force microscopy (AFM),<sup>28</sup> X-ray photoelectron spectroscopy (XPS),<sup>17</sup> and surface-enhanced Raman spectroscopy (SERS).<sup>19</sup> Among these techniques, SERS is a particularly powerful method because it is highly surface-specific, can be performed under ambient conditions, and

Received: February 2, 2021 Revised: April 9, 2021 Published: April 29, 2021





$$\begin{array}{c} \text{DDD D} \\ \text{Br} \end{array} \xrightarrow{\begin{array}{c} 2 \text{ eq.} \\ \text{H}_2\text{N} \end{array}} \xrightarrow{\begin{array}{c} 1 \text{ KHMDS, THF} \\ \text{NH HN} \end{array}} \xrightarrow{\begin{array}{c} \text{Framic acid} \\ \text{HC(OEt)_3} \\ \text{2HX} \end{array}} \xrightarrow{\begin{array}{c} \text{R}_4 \\ \text{HN} \end{array}} \xrightarrow{\begin{array}{c} \text{R}_4 \\ \text{HN} \end{array}} \xrightarrow{\begin{array}{c} \text{R}_4 \\ \text{R}_2 \text{ CO}_2, Et_2\text{O} \end{array}} \xrightarrow{\begin{array}{c} \text{R}_4 \\ \text{2. CO}_2, Et_2\text{O} \end{array}} \xrightarrow{\begin{array}{c} \text{R}_4 \\ \text{NN} \end{array}} \xrightarrow{\begin{array}{c} \text{NN} \\ \text{NN} \end{array}} \xrightarrow{\begin{array}{c} \text{NN} \\ \text{NN} \end{array}} \xrightarrow{\begin{array}{c} \text{NN} \\ \text{NN} \end{array}} \xrightarrow{\begin{array}{c} \text{R}_4 \\ \text{2. CO}_2, Et_2\text{O} \end{array}} \xrightarrow{\begin{array}{c} \text{R}_4 \\ \text{2. CO}_2, Et_2\text{O} \end{array}} \xrightarrow{\begin{array}{c} \text{NN} \\ \text{NN} \end{array}} \xrightarrow{\begin{array}{$$

Figure 2. Synthesis of imidazolinium-CO<sub>2</sub> adducts, including the deuterated analogue (3).

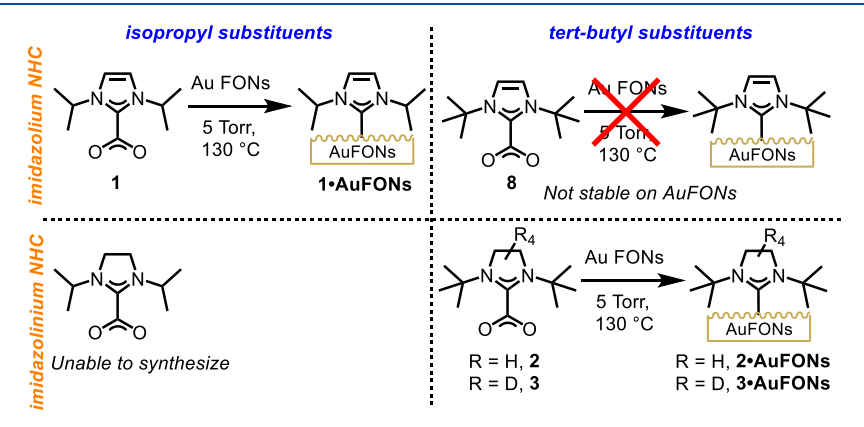


Figure 3. Protocol for depositing NHC-CO<sub>2</sub> adducts onto gold substrates. While AuFONs are shown in this scheme, the same procedure is also used for flat gold mirrors. This work examines the deposition of 1, 2, and 3 on Au surfaces. Chechik and co-workers previously demonstrated that surfaces obtained from 8 are not stable.<sup>57</sup> The imidazolinium NHC with isopropyl side groups (bottom left) presented synthetic challenges and could not be isolated (*vide infra*).

exploits a molecule's unique vibrational fingerprint to determine the structure of the surface-bound molecules. <sup>29,30</sup> The SERS spectral features for imidazolium and benzimidazolium NHCs on gold film-over-nanosphere (AuFON) substrates have been well characterized previously by our groups through a dual experimental and theoretical approach. <sup>25</sup>

This paucity of NHC motifs is unfortunate because synthetic NHC chemistry has achieved an extraordinary range in structure and application beyond these two basic designs. In the field of organometallic homogenous catalysis, NHC ligands have noticeably shifted from imidazolium NHCs to include a wider array of NHC motifs which often lead to improvements in catalytic activity. A similar shift to different NHC structures on gold surfaces may significantly improve nanosystem stability and introduce an array of new applications to carbene-functionalized surfaces (Figure 1).

Less-explored NHCs offer two promising advantages over imidazolium and benzimidazolium NHC ligands. First, they exhibit stronger metal-ligand bonds due to either increased  $\sigma$ donor strength or  $\pi$ -backbonding.<sup>35</sup> Stronger bonds could yield a more stable ligand surface and minimize the potential for desorption into the supernatant, which is particularly important for applications involving tethered catalysts<sup>36,37</sup> or biological media. 38,39 Second, these different carbene ligands, specifically imidazolinium NHCs, offer the synthetic possibility for appending two different functionalities in C2-symmetry onto the carbene backbone. Thus, a host of chiral NHC ligands may be achievable, yielding novel enantiomeric surfaces. Although chiral NHCs have been synthesized for many homogenous reactions, 40-42 very few examples of such NHC surfaces exist, and the ones that do often involve complex monolayers or surfaces where the chiral group is

distanced considerably from the surface. <sup>21,43,44</sup> For example, chiral molecule detection schemes sometimes rely on thiol-binding ligands that are limited by the thiol linker's stability. <sup>45–47</sup> In addition to the potentially increased stability, C<sub>2</sub>-symmetric imidazolinium NHC coatings may allow for the chiral moiety to be closer to the surface, which is integral for techniques relying on the signal enhancement offered by surface plasmon resonances. <sup>48–50</sup> Despite these potential advantages, to date, only one additional carbene motif has been reported on a gold surface, 1,3-dimesityl-imidazolinium; however, this surface was only characterized by XPS. <sup>17</sup>

In this work, we prepare NHC-coated gold surfaces with either a standard (*i.e.*, imidazolium) or less-explored (*i.e.*, imidazolinium) NHC ligand *via* a CO<sub>2</sub> adduct deposition method, showcasing the first successful deposition of a NHC ligand that does not include imidazolium or benzimidazolium moieties on a SERS-active substrate. Comparing the stability of these surface-bound molecules under extreme pH conditions, we find a clear stability enhancement under acidic conditions for the imidazolinium NHC. More generally, this research highlights the deposition, characterization, and stability of imidazolinium and points to a promising future for different NHC ligands on metal surfaces.

#### 2. EXPERIMENTAL SECTION

**2.1. Materials and General Considerations.** All glassware for air- and water-sensitive reactions were dried at 170 °C overnight before use. All reactions were stirred vigorously with magnetic stirrers. Syntheses of the NHC-CO<sub>2</sub> adducts were performed under a dry dinitrogen atmosphere with the use of either a glovebox or standard Schlenk techniques. Solvents used under the N<sub>2</sub> atmosphere were dried on an Innovative Technologies (Newburyport, MA) Pure Solv MD-7 solvent purification system, degassed by three freeze-pumpthaw cycles on a Schlenk line to remove dioxygen, and stored over

activated 4 Å molecular sieves prior to use. Celite was dried at 240 °C under vacuum overnight and stored in a dinitrogen glovebox. Compounds  $\mathbf{1}_{1}^{2.5}$   $\mathbf{2}_{1}^{51}$   $\mathbf{4}_{1}^{52}$   $\mathbf{6}_{1}^{52}$  and  $\mathbf{8}^{53}$  were prepared following previous literature procedures (Figures 2, 3). All other compounds were purchased from commercial vendors at the highest available purity and used without any further purification.

Glass slides were purchased from VWR International. Polystyrene spheres ( $d=600\,\text{nm}$ ) were purchased from Sigma-Aldrich. Gold (99.99% pure) and chromium (99.95% pure) pieces were purchased from the Kurt J. Lesker Company. Chemicals were used as received without further purification.

2.2. Synthesis of Compound 3. The NHC-CO<sub>2</sub> adduct of 1,3di-tert-butyl-4,5-tetradeuteroimidazolinium bromide, 7, was prepared following a slightly modified method of Buchmeiser.5 potassium bis(trimethylsilyl)amide (0.3560 g, 1.785 mmol) and tetrahydrofuran (12 mL) were added to a vial containing 7 (0.4774 g, 1.786 mmol) and was stirred overnight at RT in a glovebox. The solvent was then removed under vacuum. The residue was then extracted with diethyl ether (15 mL) and filtered into a Schlenk flask over a short Celite plug to remove solid KBr formed during the reaction. The Schlenk flask containing the free carbene in diethyl ether was removed from the glovebox and CO2 gas was added to the flask under an air-free setup and stirred for 15 min. After the addition of CO2, a white solid immediately formed. The reaction vessel was placed under vacuum and returned to the glovebox. The suspension was filtered over a fine porosity frit and washed with 10 mL of diethyl ether. The solid was dried under vacuum for no more than 5 min to give a white powder. Yield: 0.292 g, 71.0%. <sup>1</sup>H NMR (CD<sub>2</sub>Cl<sub>2</sub>, 499.74 MHz):  $\delta$  1.46 (s, 18H). <sup>13</sup>C NMR (CD<sub>2</sub>Cl<sub>2</sub>, 125.66 MHz):  $\delta$  164.63, 159.38, 58.45, 44.28 (pent, I = 22.54 Hz), 28.25. IR: 2973, 2238, 1669, 1571, 1484, 1407, 1390, 1377, 1366, 1322, 1262, 1230, 1194, 1137, 1088, 1051, 991, 978, 946, 930, 909, 892, 816, 770, 725 cm<sup>-1</sup>.

**2.3.** Synthesis of Compound 5. N,N'-di-tert-butyl-( $d_4$ )-ethylenediamine dihydrobromic acid, 5, was prepared using a modification of a previously reported literature method. A 20 mL scintillation vial was charged with a stir bar,  $d_4$ -dibromoethylenediamine (1.312 g, 6.837 mmol), tert-butylamine (3.952 mL, 37.61 mmol), 2 mL of hexane, and 2 mL of DI water and capped with a Teflon screw cap. The solution was stirred overnight at 110 °C. The reaction was cooled to RT and, upon cooling, a white precipitate formed. The supernatant was decanted off and the solid was washed with 10 mL of hexane and dried under vacuum to give a white tacky solid. Yield: 1.95 g, 84.4%. H NMR (CDCl<sub>3</sub>, 499.74 MHz): δ 5.58 (s, 4H), 1.41 (s, 9H), 1.29 (s, 9H). CDCl<sub>3</sub>, 125.66 MHz): δ 54.46, 52.33, 39.71 (pent, J = 21.06), 29.06, 27.74. IR: 3380, 3217, 2966, 2891, 2838, 2770, 2678, 2584, 2485, 2409, 2222, 2091, 2033, 1621, 1501, 1479, 1451, 1400, 1377, 1363, 1298, 1246, 1210, 1136, 1108, 1062, 1042, 986, 968, 936, 880, 762, 730 cm<sup>-1</sup>.

**2.4. Synthesis of Compound 7.** Compound 7 was prepared following the method of Barry. <sup>52</sup> A 100 mL round-bottom flask was charged with a stir bar, compound **5** (1.073 g, 3.173 mmol), triethyl orthoformate (18 mL, 0.1082 mol), and seven drops of formic acid and was stirred for 24 h at 130 °C. The reaction was then cooled to RT and 40 mL of diethyl ether was added. The resulting suspension was filtered over a medium porosity frit and washed with an additional 30 mL of ether. The solid was dried under vacuum to give a white powder. Yield: 0.481 g, 56.8%. <sup>1</sup>H NMR (CD<sub>2</sub>Cl<sub>2</sub>, 499.74 MHz): δ 8.53 (s, 1H), 1.49 (s, 18H). <sup>13</sup>C NMR (CD<sub>2</sub>Cl<sub>2</sub>, 150.81 MHz): δ 153.78, 57.31, 44.99 (pent, J = 22.80 Hz), 28.26. IR: 2971, 2917, 2875, 2236, 2128, 1613, 1472, 1459, 1402, 1376, 1368, 1314, 1280, 1233, 1205, 1140, 1120, 1082, 1044, 981, 920, 887, 861, 825, 789 cm<sup>-1</sup>.

**2.5.** Au NHC Substrate Preparation. First, gold mirrors and AuFONs were prepared for the XPS and SERS measurements, respectively. Glass slides were thoroughly cleaned using a Plasma Prepp II SPI  $O_2$  plasma instrument. Following a previously reported synthesis procedure for AuFONs,  $^{55}$  a compact monolayer of polystyrene spheres (d=600 nm) was deposited onto a glass slide. Then, polystyrene-coated slides and bare glass slides were inserted into a physical vapor deposition chamber (Nano 36, Kurt J. Lesker)

whereby a chromium adhesion layer ( $\sim$ 5 nm) was evaporated onto the slides followed by a thick gold layer ( $\sim$ 200 nm), yielding AuFONs and gold mirrors, respectively.

To prepare the NHC-coated substrates, a previously reported protocol was followed. <sup>19</sup> First, the substrate (*e.g.*, mirror or AuFONs) was placed in an Erlenmeyer flask with the gold layer facing up. The NHC-CO<sub>2</sub> adduct powder was carefully placed on top of the exposed gold surface. The flask was connected to a vacuum line, achieving a base pressure of 5 torr before immersion in a 130 °C oil bath. Upon heating, the CO<sub>2</sub> group leaves, exposing the free carbene to readily react with the gold surface. After approximately 10 min, the reaction is completed with no visible powder remaining on the surface.

**2.6. Instrumentation.** Solution <sup>1</sup>H nuclear magnetic resonance (NMR) spectroscopy and <sup>13</sup>C NMR spectroscopy were performed on a Varian VNMRS 500 MHz narrow-bore broadband system and Varian VNMRS 600 MHz narrow-bore broadband system at 298 K. All <sup>1</sup>H and <sup>13</sup>C shifts were referenced to the residual solvent. Infrared spectra were collected on a Thermo Scientific Nicolet iS10 with a Smart iTR accessory for attenuated total reflectance (ATR) using the neat compounds.

XPS measurements were obtained with a PHI VersaProbe II surface analysis instrument (Physical Electronics). The instrument operates under ultrahigh vacuum with a monochromatic Al K $\alpha$ X-ray source (photon energy = 1486.6 eV). High-resolution spectra were obtained using a 23.50 eV pass energy. All resulting spectra were calibrated versus the binding energy of sp³ hybridized carbon (C 1s = 284.8 eV) and background-subtracted according to the Shirley algorithm.  $^{56}$ 

SERS spectra were recorded using a custom-built Raman spectrometer equipped with a 633 nm HeNe laser (Thor Labs). The laser beam was aligned into an inverted microscope objective (Nikon, 20×, NA = 0.5) with approximately 600  $\mu$ W of power at the sample. Acquisitions were approximately 3 min. The resulting backscattered photons were passed through a Rayleigh rejection filter (Semrock) prior to detection in a dispersive spectrometer (Acton SP2300, Princeton Instruments, 1200 g mm<sup>-1</sup>) equipped with a backilluminated deep depletion CCD (PIXIS, Spec-10, Princeton Instruments). The resulting scans were recorded with Winspec 32 software (Princeton Instruments). For each sample, scans were taken at three different positions on the substrate to ensure signal reproducibility. The acquired spectra were background-subtracted (Multipeak Fitting 2.0 Package) and graphed using IGOR Pro (Wavemetrics).

### 3. RESULTS AND DISCUSSION

Synthesis of the imidazolinium– $CO_2$  adduct (Figure 2, 2) and imidazolium-CO<sub>2</sub> adduct (Figure 3, 1) was completed following previous literature procedures. <sup>25,51</sup> Synthesis of the deuterated imidazolinium-CO2 adduct (Figure 2, 3) was completed by modifying previous protocols. First, following the method of Jiao with slight modifications,  $d_4$ -dibromoethylenediamine was reacted with tert-butylamine at reflux.54 The resulting solid was collected and washed with hexanes and dried to give N,N'-di-tert-butyl- $(d_4)$ -ethylenediamine dihydrobromic acid, 5. Compound 5 was then reacted with triethyl orthoformate and a catalytic amount of formic acid at reflux following the method of Barry. 52 Upon cooling, the solution was titrated with diethyl ether, and the resulting precipitate was filtered and washed with additional ether and dried to give 1,3di-tert-butyl-4,5-tetradeuteroimidazolinium bromide, 7. The deuterated  $CO_2$  adduct, 3, was synthesized following the method of Buchmeiser. The imidazolinium salt, 7, was deprotonated with KHMDS. The solution was then dried and the free carbene of 7 was extracted with diethyl ether and placed into a Schlenk flask. CO2 gas was then added to the flask under a N<sub>2</sub> atmosphere, resulting in the immediate

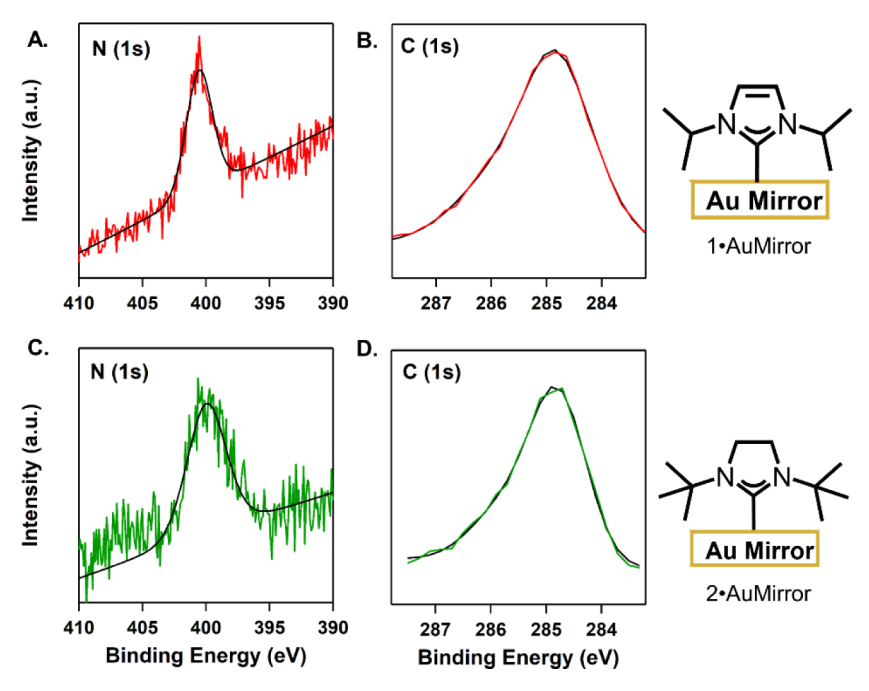


Figure 4. XPS analyses of Au mirrors functionalized with ligands 1 (red traces) and 2 (green traces) along with the overall fits (black traces). (A) N 1s peak is at 400.45 eV, (B) C 1s peak is at 284.85 eV, (C) N 1s peak is at 399.92 eV, and (D) C 1s peak is at 284.91 eV.

formation of a precipitate. The reaction flask was brought into the glovebox and filtered. The solid was then washed with diethyl ether and dried under vacuum for no longer than 5 min to prevent the loss of CO<sub>2</sub>, to give pure 3 in 71% yield.

The  $CO_2$  adducts, 1–3, were characterized with  $^1H$  and  $^{13}C$  NMR spectroscopy. A successful adduct formation is indicated by the disappearance of the  $C_2$  C–H signal between 8 and 10 ppm in  $^1H$  NMR as well as the appearance of a  $CO_2$  carbon peak around 155 and 163 ppm in  $^{13}C$  NMR for the imidazolium 1 and imidazoliniums 2–3 respectively (Figures S1–S10). The  $^1H$  NMR of 3 shows no loss of deuteration content in the synthesis of the final  $CO_2$  adduct.

Metal film-over-nanospheres (FONs) were employed as SERS substrates due to their relatively straightforward preparation, high stability, and uniform intensity enhancement. SS,58 Scanning electron microscopy (SEM) images of the prepared AuFONs display a compact layer of gold-coated polystyrene spheres (Figure S11). Air-stable NHC-CO<sub>2</sub> adducts are optimal for this study because they offer a facile approach for depositing NHC ligands onto solid surfaces, particularly gold. With CO<sub>2</sub> as a leaving group, the NHC directly attaches to the surface without needing additional reagents, which reduces the potential for fouling. For this approach to be successful, both the NHC-CO<sub>2</sub> adducts must be able to be synthesized and need to react with AuFONs to form a stable surface.

We began by pursuing isopropyl substituents because these have shown great stability with benzimidazolium NHCs on solid surfaces and nanoparticles (Figure 1B). 17–19 Compound 1, the imidazolium NHC–CO<sub>2</sub> adduct powder, was placed directly on top of the gold surface and was heated to 130 °C *in vacuo* (Figure 3, top left) resulting in 1·AuFONs. 19 Although we attempted the synthesis of the imidazolinium NHC–CO<sub>2</sub> adduct with isopropyl groups as the N-substituents (Figure 3, bottom left), the product could not be isolated due to high solubility in all tested solvents. The closest match to an isopropyl group that affords stable NHC–CO<sub>2</sub> adducts is

NHCs with *tert*-butyl substituents. The imidazolinium NHC–CO<sub>2</sub> adduct, **2**, was previously synthesized, <sup>51</sup> and we appended it to AuFONs in the same manner as **1**, yielding **2·AuFONs** (Figure 3, bottom right). Its deuterated analogue, **3**, was also successfully deposited. We also synthesized the di-*tert*-butyl imidazolium–CO<sub>2</sub> adduct, **8**, <sup>53</sup> starting from commercially available di-*tert*-butyl imidazolium chloride as a direct comparison to the imidazolinium (Figure 3, top right). Unfortunately, the reaction to append **8** to the AuFONs surface was not successful, which is not unexpected as Chechik and co-workers previously reported that **8** was not stable on gold nanoparticles and leached into solution in less than 12 h <sup>57</sup>

Given that both the NHCs' nitrogen substituents and the electronics of the NHCs are distinct, it is important to determine whether the differences in stability are due to electronic or steric effects. Fortunately, the steric parameters for NHCs are well known and often described in terms of buried volume, which is analogous to the cone angle for phosphines. NHC 1 has a buried volume of 27.4% and its benzimidazolium variant which we previously reported on AuFONs (1 in ref 19) has a buried volume of 27.9%. Switching to the *tert*-butyl substituents increases the buried volume significantly (36.2% for 2 and 35.5% for 8). Note that in both cases, changing the electronic structure of the NHC (*i.e.*, saturated *vs* unsaturated) does not change the steric parameters of buried volume significantly.

We also synthesized 1 and 2 Au NHC surfaces on gold mirrors, and they were characterized with XPS. Flat gold mirrors were used to avoid any residual signal from polystyrene. A control spectrum of the gold mirror before NHC deposition exhibits no observable N 1s signal (Figure S12). High-resolution N 1s spectra for imidazolinium and imidazolium present one symmetric peak at 399.92 and 400.45 eV, respectively (Figure 4). This slight variance in the peak position suggests the presence of unique chemical environments for two different molecular species. Hamers and co-

workers, 62 for example, observed that nitrogen-containing moieties on Si(001) surfaces exhibited a 1 eV shift in the N 1s peak between aromatic pyrrole and its completely saturated analogue pyrrolidine, claiming that the higher binding energy is a direct result of the retained aromaticity of pyrrole on the surface. Therefore, the  $\sim$ 0.5 eV shift to a higher binding energy may be due to the higher degree of aromaticity in the imidazolium moiety. High-resolution C 1s spectra for imidazolinium and imidazolium both yield peaks at around 285 eV (Figure 4). However, the broadness of the peaks indicates multiple chemical states which cannot be easily differentiated as the complex carbon-carbon and carbonnitrogen environments give rise to multiple peaks between 284–285 and 285–288 eV, respectively. 63 Most importantly for the current work, these N, C, and Au (Figure S13) peak values are all consistent with literature reports for NHC ligands bonded directly to the gold surface. 17,18,27,64 Therefore, XPS indicates the presence of intact carbene molecules on the gold surface.

Figure 5 (top row) presents SERS spectra of 1·AuFONs and 2·AuFONs directly following CO<sub>2</sub> adduct deposition. 1·

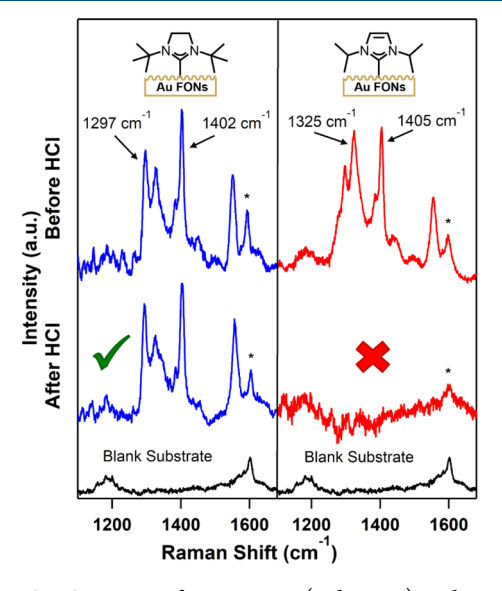


Figure 5. SERS spectra of 1·AuFONs (red traces) and 2·AuFONs (blue traces) before (top row) and after (middle row) exposure to 1 M HCl for 24 h. The bottom row is a blank SERS spectrum of the AuFON substrate. Peaks marked with an asterisk are from the substrate.

**AuFONs** exhibit characteristic, dominant peaks at 1325 and 1405 cm<sup>-1</sup>, which are primarily attributed to the isopropyl side groups interacting strongly with the NHC nitrogens. Due to the nuanced vibrational modes that SERS can reveal, we can be confident that our resulting spectra for **1**·**AuFONs** are, in fact, distinct from those of **2**·**AuFONs** which have two dominating peaks at 1297 and 1402 cm<sup>-1</sup>. This deposition protocol and the corresponding SERS signature for **2**·**AuFONs** are found to be highly reproducible.

As an additional test, the deuterated analogue of the imidazolinium NHC ligand was affixed to AuFONs, forming **3**· **AuFONs**. By substituting the hydrogens on the NHC backbone with deuterium, the vibrational signature changes significantly (Figure S14). Previously reported  $d_2$ -imidazolium spectra have dominant peaks at 1303 and 1401 cm<sup>-1,25</sup> whereas **3**·**AuFONs** exhibit a dominant peak at 1350 cm<sup>-1</sup>.

The deposition and SERS analysis were performed in triplicate to ensure that the spectrum was consistent.

Although benzimidazolium NHCs adhere to Au surfaces very well, 17,19,65 similar tests have not been as extensively conducted for imidazolium NHCs and no tests of imidazolinium have been undertaken. We postulated that the imidazolinium NHC ligand, 2, would exhibit enhanced stability in acid due to increased  $\sigma$ -donation and because it would not be prone to the electrophilic attack at the 4 and 5 positions on the ring in the same manner as imidazole NHC, 1.66 Indeed, a few unsaturated imidazoliums have been converted to saturated imidazoliniums by the addition of a strong acid.67,68 Upon submerging the respective NHC-coated AuFONs in hydrochloric acid (1 M) for 24 h, we observed a complete degradation of the imidazolium NHC signal (Figure 5, right), whereas the imidazolinium variant is unchanged (Figure 5, left). These results demonstrate a limitation for one of the two most commonly used NHC ligands on gold surfaces: stability toward strong acids. It should be noted that while the tert-butyl group provides additional steric stability to the ligand, we believe that the primary degradation mechanism is via an electrophilic attack on the imidazolium ring as described above. The rationale behind this is that the buried volumes for the imidazolium and previously studied benzimidazolium NHCs are almost identical (see above), but the benzimidazolium, which is not susceptible to electrophilic attack, is stable in acid. 19 In addition, we find that both imidazolium and imidazolinium are stable when exposed to strongly basic conditions (1 M KOH, 24 h) or water as a control (Figures S15 and S16). All stability tests were performed in triplicate.

#### 4. CONCLUSIONS

We report the first detailed exploration of imidazolinium NHCs, including deposition from the CO<sub>2</sub> adduct, demonstrating enhanced stability under acidic conditions compared to traditional imidazolium. In addition to SERS and XPS characterization of the imidazolinium surfaces, a deuterated isotopologue of imidazolinium was synthesized for the first time. We envision this work promoting the broader use of different carbene motifs on gold surfaces and future investigations could include synthesizing chiral moieties on the imidazolinium backbone for surface detection and depositing these carbenes on aqueous nanoparticles *via* gold complexes.

#### ASSOCIATED CONTENT

## Supporting Information

The Supporting Information is available free of charge at https://pubs.acs.org/doi/10.1021/acs.langmuir.1c00314.

NMR and IR characterization for the NHC-CO<sub>2</sub> adducts, SEM characterization of the SERS substrate, additional XPS analyses and SERS data for the deuterated isotopologues, and stability tests (PDF)

### AUTHOR INFORMATION

# **Corresponding Authors**

David M. Jenkins — Department of Chemistry, University of Tennessee, Knoxville 37996, Tennessee, United States; Email: jenkins@ion.chem.utk.edu

Jon P. Camden – Department of Chemistry and Biochemistry, University of Notre Dame, South Bend 46556, Indiana, *United States;* orcid.org/0000-0002-6179-2692; Email: jon.camden@nd.edu

#### **Authors**

Lindy M. Sherman — Department of Chemistry and Biochemistry, University of Notre Dame, South Bend 46556, Indiana, United States; orcid.org/0000-0003-2435-8886 Shelby L. Strausser — Department of Chemistry, University of Tennessee, Knoxville 37996, Tennessee, United States Rowan K. Borsari — Department of Chemistry, University of Tennessee, Knoxville 37996, Tennessee, United States

Complete contact information is available at: https://pubs.acs.org/10.1021/acs.langmuir.1c00314

#### **Author Contributions**

The article was written through contributions of all authors. All authors have given approval to the final version of the article. L.M.S. and S.L.S. contributed equally.

#### **Notes**

The authors declare no competing financial interest.

### ACKNOWLEDGMENTS

This material is based on work supported by the National Science Foundation under grant numbers CHE-1709881 (L.M.S. and J.P.C.) and CHE-1709468 (S.L.S, R.K.B. and D.M.J.). Any opinions, findings, and conclusions or recommendations expressed in this material are those of the authors and do not necessarily reflect the views of the National Science Foundation. L. M. S. acknowledges support from the Arthur J. Schmitt Foundation. J.P.C. and L.M.S. thank the ND Energy Materials Characterization Facility for use of their XPS instrument. L.M.S. is grateful for the use of the  $\rm O_2$  Plasma Instrument in the Paul Bohn Lab for cleaning the glass slides. L.M.S. would also like to thank Nathan Dominique for assistance in acquiring the scanning electron microscopy image and the Notre Dame Integrated Imaging Facility for use of their instrument.

# REFERENCES

- (1) Engel, S.; Fritz, E.-C.; Ravoo, B. J. New trends in the functionalization of metallic gold: from organosulfur ligands to N-heterocyclic carbenes. *Chem. Soc. Rev.* **2017**, *46*, 2057–2075.
- (2) Goddard, Z. R.; Marín, M. J.; Russell, D. A.; Searcey, M. Active targeting of gold nanoparticles as cancer therapeutics. *Chem. Soc. Rev.* **2020**, *49*, 8774–8789.
- (3) Heuer-Jungemann, A.; Feliu, N.; Bakaimi, I.; Hamaly, M.; Alkilany, A.; Chakraborty, I.; Masood, A.; Casula, M. F.; Kostopoulou, A.; Oh, E.; Susumu, K.; Stewart, M. H.; Medintz, I. L.; Stratakis, E.; Parak, W. J.; Kanaras, A. G. The Role of Ligands in the Chemical Synthesis and Applications of Inorganic Nanoparticles. *Chem. Rev.* 2019, 119, 4819–4880.
- (4) Smith, C. A.; Narouz, M. R.; Lummis, P. A.; Singh, I.; Nazemi, A.; Li, C.-H.; Crudden, C. M. N-Heterocyclic Carbenes in Materials Chemistry. *Chem. Rev.* **2019**, *119*, 4986–5056.
- (5) Sun, F.; Galvan, D. D.; Jain, P.; Yu, Q. Multi-functional, thiophenol-based surface chemistry for surface-enhanced Raman spectroscopy. *Chem. Commun.* **2017**, *53*, 4550–4561.
- (6) Zhukhovitskiy, A. V.; MacLeod, M. J.; Johnson, J. A. Carbene Ligands in Surface Chemistry: From Stabilization of Discrete Elemental Allotropes to Modification of Nanoscale and Bulk Substrates. *Chem. Rev.* **2015**, *115*, 11503–11532.
- (7) Li, Y.; Huang, J.; McIver, R. T.; Hemminger, J. C. Characterization of thiol self-assembled films by laser desorption Fourier transform mass spectrometry. *J. Am. Chem. Soc.* **1992**, *114*, 2428–2432.

- (8) Schoenfisch, M. H.; Pemberton, J. E. Air Stability of Alkanethiol Self-Assembled Monolayers on Silver and Gold Surfaces. *J. Am. Chem. Soc.* **1998**, *120*, 4502–4513.
- (9) Willey, T. M.; Vance, A. L.; van Buuren, T.; Bostedt, C.; Terminello, L. J.; Fadley, C. S. Rapid degradation of alkanethiol-based self-assembled monolayers on gold in ambient laboratory conditions. *Surf. Sci.* **2005**, *576*, 188–196.
- (10) Andrieux-Ledier, A.; Tremblay, B.; Courty, A. Stability of Self-Ordered Thiol-Coated Silver Nanoparticles: Oxidative Environment Effects. *Langmuir* **2013**, *29*, 13140–13145.
- (11) Bhatt, N.; Huang, P.-J. J.; Dave, N.; Liu, J. Dissociation and Degradation of Thiol-Modified DNA on Gold Nanoparticles in Aqueous and Organic Solvents. *Langmuir* **2011**, *27*, 6132–6137.
- (12) Wu, Y.; Lian, J.; Gonçales, V. R.; Pardehkhorram, R.; Tang, W.; Tilley, R. D.; Gooding, J. J. Patterned Molecular Films of Alkanethiol and PLL-PEG on Gold-Silicate Interfaces: How to Add Functionalities while Retaining Effective Antifouling. *Langmuir* **2020**, *36*, 5243–5250.
- (13) Zhang, J.; Léonard, D.; Yeromonahos, C.; Mazurczyk, R.; Géhin, T.; Monfray, S.; Chevolot, Y.; Cloarec, J.-P. Orthogonal Chemical Functionalization of Au/SiO2/TiW Patterned Substrates. *Langmuir* **2020**, *36*, 14960–14966.
- (14) Zhang, D.; Hao, R.; Zhang, L.; You, H.; Fang, J. Ratiometric Sensing of Polycyclic Aromatic Hydrocarbons Using Capturing Ligand Functionalized Mesoporous Au Nanoparticles as a Surface-Enhanced Raman Scattering Substrate. *Langmuir* **2020**, *36*, 11366–11373
- (15) Arroyo-Currás, N.; Somerson, J.; Vieira, P. A.; Ploense, K. L.; Kippin, T. E.; Plaxco, K. W. Real-time measurement of small molecules directly in awake, ambulatory animals. *Proc. Natl. Acad. Sci. U.S.A.* **2017**, *114*, 645.
- (16) Li, H.; Dauphin-Ducharme, P.; Arroyo-Currás, N.; Tran, C. H.; Vieira, P. A.; Li, S.; Shin, C.; Somerson, J.; Kippin, T. E.; Plaxco, K. W. A Biomimetic Phosphatidylcholine-Terminated Monolayer Greatly Improves the In Vivo Performance of Electrochemical Aptamer-Based Sensors. *Angew. Chem., Int. Ed.* **2017**, *56*, 7492–7495.
- (17) Crudden, C. M.; Horton, J. H.; Ebralidze, I. I.; Zenkina, O. V.; McLean, A. B.; Drevniok, B.; She, Z.; Kraatz, H.-B.; Mosey, N. J.; Seki, T.; Keske, E. C.; Leake, J. D.; Rousina-Webb, A.; Wu, G. Ultra stable self-assembled monolayers of N-heterocyclic carbenes on gold. *Nat. Chem.* **2014**, *6*, 409.
- (18) DeJesus, J. F.; Sherman, L. M.; Yohannan, D. J.; Becca, J. C.; Strausser, S. L.; Karger, L. F. P.; Jensen, L.; Jenkins, D. M.; Camden, J. P. A Benchtop Method for Appending Protic Functional Groups to N-Heterocyclic Carbene Protected Gold Nanoparticles. *Angew. Chem., Int. Ed.* **2020**, *59*, 7585–7590.
- (19) DeJesus, J. F.; Trujillo, M. J.; Camden, J. P.; Jenkins, D. M. N-Heterocyclic Carbenes as a Robust Platform for Surface-Enhanced Raman Spectroscopy. *J. Am. Chem. Soc.* **2018**, *140*, 1247–1250.
- (20) MacLeod, M. J.; Johnson, J. A. PEGylated N-Heterocyclic Carbene Anchors Designed To Stabilize Gold Nanoparticles in Biologically Relevant Media. J. Am. Chem. Soc. 2015, 137, 7974—7977
- (21) Nguyen, D. T.; Freitag, M.; Gutheil, C.; Sotthewes, K.; Tyler, B. J.; Böckmann, M.; Das, M.; Schlüter, F.; Doltsinis, N. L.; Arlinghaus, H. F.; Ravoo, B. J.; Glorius, F. An Arylazopyrazole-Based N-Heterocyclic Carbene as a Photoswitch on Gold Surfaces: Light-Switchable Wettability, Work Function, and Conductance. *Angew. Chem., Int. Ed.* **2020**, *59*, 13651–13656.
- (22) Li, Z.; Munro, K.; Ebralize, I. I.; Narouz, M. R.; Padmos, J. D.; Hao, H.; Crudden, C. M.; Horton, J. H. N-Heterocyclic Carbene Self-Assembled Monolayers on Gold as Surface Plasmon Resonance Biosensors. *Langmuir* **2017**, *33*, 13936–13944.
- (23) Mayall, R. M.; Smith, C. A.; Hyla, A. S.; Lee, D. S.; Crudden, C. M.; Birss, V. I. Ultrasensitive and Label-Free Detection of the Measles Virus Using an N-Heterocyclic Carbene-Based Electrochemical Biosensor. *ACS Sens.* **2020**, *5*, 2747–2752.

- (24) Roland, S.; Ling, X.; Pileni, M.-P. N-Heterocyclic Carbene Ligands for Au Nanocrystal Stabilization and Three-Dimensional Self-Assembly. *Langmuir* **2016**, *32*, 7683–7696.
- (25) Trujillo, M. J.; Strausser, S. L.; Becca, J. C.; DeJesus, J. F.; Jensen, L.; Jenkins, D. M.; Camden, J. P. Using SERS To Understand the Binding of N-Heterocyclic Carbenes to Gold Surfaces. *J. Phys. Chem. Lett.* **2018**, *9*, 6779–6785.
- (26) Voutchkova, A. M.; Feliz, M.; Clot, E.; Eisenstein, O.; Crabtree, R. H. Imidazolium Carboxylates as Versatile and Selective N-Heterocyclic Carbene Transfer Agents: Synthesis, Mechanism, and Applications. J. Am. Chem. Soc. 2007, 129, 12834–12846.
- (27) Wang, G.; Rühling, A.; Amirjalayer, S.; Knor, M.; Ernst, J. B.; Richter, C.; Gao, H.-J.; Timmer, A.; Gao, H.-Y.; Doltsinis, N. L.; Glorius, F.; Fuchs, H. Ballbot-type motion of N-heterocyclic carbenes on gold surfaces. *Nat. Chem.* **2017**, *9*, 152–156.
- (28) Nguyen, D. T.; Freitag, M.; Körsgen, M.; Lamping, S.; Rühling, A.; Schäfer, A. H.; Siekman, M. H.; Arlinghaus, H. F.; van der Wiel, W. G.; Glorius, F.; Ravoo, B. J. Versatile Micropatterns of N-Heterocyclic Carbenes on Gold Surfaces: Increased Thermal and Pattern Stability with Enhanced Conductivity. *Angew. Chem., Int. Ed.* 2018, 57, 11465–11469.
- (29) Haynes, C. L.; McFarland, A. D.; Van Duyne, R. P. Surface-Enhanced Raman Spectroscopy. *Anal. Chem.* **2005**, *77*, 338A–346A.
- (30) Schlücker, S. Surface-Enhanced Raman Spectroscopy: Concepts and Chemical Applications. *Angew. Chem., Int. Ed.* **2014**, *53*, 4756–4795.
- (31) Hopkinson, M. N.; Richter, C.; Schedler, M.; Glorius, F. An overview of N-heterocyclic carbenes. *Nature* **2014**, *510*, 485–496.
- (32) Bakker, A.; Freitag, M.; Kolodzeiski, E.; Bellotti, P.; Timmer, A.; Ren, J.; Schulze Lammers, B.; Moock, D.; Roesky, H. W.; Mönig, H.; Amirjalayer, S.; Fuchs, H.; Glorius, F. An Electron-Rich Cyclic (Alkyl)(Amino)Carbene on Au(111), Ag(111), and Cu(111) Surfaces. Angew. Chem., Int. Ed. 2020, 59, 13643–13646.
- (33) Marx, V. M.; Sullivan, A. H.; Melaimi, M.; Virgil, S. C.; Keitz, B. K.; Weinberger, D. S.; Bertrand, G.; Grubbs, R. H. Cyclic Alkyl Amino Carbene (CAAC) Ruthenium Complexes as Remarkably Active Catalysts for Ethenolysis. *Angew. Chem., Int. Ed.* **2015**, *54*, 1919–1923
- (34) Melaimi, M.; Jazzar, R.; Soleilhavoup, M.; Bertrand, G. Cyclic (Alkyl)(amino)carbenes (CAACs): Recent Developments. *Angew. Chem., Int. Ed.* **2017**, *56*, 10046–10068.
- (35) Back, O.; Henry-Ellinger, M.; Martin, C. D.; Martin, D.; Bertrand, G. 31P NMR Chemical Shifts of Carbene–Phosphinidene Adducts as an Indicator of the π-Accepting Properties of Carbenes. *Angew. Chem., Int. Ed.* **2013**, *52*, 2939–2943.
- (36) Murakami, K.; Tanaka, Y.; Sakai, R.; Hisai, Y.; Hayashi, S.; Mizutani, Y.; Higo, T.; Ogo, S.; Seo, J. G.; Tsuneki, H.; Sekine, Y. Key factor for the anti-Arrhenius low-temperature heterogeneous catalysis induced by H+ migration: H+ coverage over support. *Chem. Commun.* **2020**, *56*, 3365–3368.
- (37) Zhao, F.; Bhanage, B. M.; Shirai, M.; Arai, M. Heck Reactions of Iodobenzene and Methyl Acrylate with Conventional Supported Palladium Catalysts in the Presence of Organic and/and Inorganic Bases without Ligands. *Chem.—Eur J.* **2000**, *6*, 843–848.
- (38) Borzenkov, M.; Chirico, G.; D'Alfonso, L.; Sironi, L.; Collini, M.; Cabrini, E.; Dacarro, G.; Milanese, C.; Pallavicini, P.; Taglietti, A.; Bernhard, C.; Denat, F. Thermal and Chemical Stability of Thiol Bonding on Gold Nanostars. *Langmuir* 2015, 31, 8081–8091.
- (39) Flynn, N. T.; Tran, T. N. T.; Cima, M. J.; Langer, R. Long-Term Stability of Self-Assembled Monolayers in Biological Media. *Langmuir* **2003**, *19*, 10909–10915.
- (40) Ma, J.-T.; Cheng, Y. Construction of enantiopure imine bridged benzo[ $\epsilon$ ] azepinones by a silver(i) and chiral N-heterocyclic carbene multicatalytic reaction sequence of N'-(2-alkynylbenzylidene)-hydrazides and cyclopropanecarbaldehydes. *Org. Chem. Front.* **2020**, 7, 3459–3467.
- (41) Singha, S.; Patra, T.; Daniliuc, C. G.; Glorius, F. Highly Enantioselective [5 + 2] Annulations through Cooperative N-

- Heterocyclic Carbene (NHC) Organocatalysis and Palladium Catalysis. J. Am. Chem. Soc. 2018, 140, 3551-3554.
- (42) Thongpaen, J.; Schmid, E. T.; Toupet, L.; Dorcet, V.; Mauduit, M.; Baslé, O. Directed ortho C–H borylation catalyzed using Cp\*Rh(iii)–NHC complexes. *Chem. Commun.* **2018**, *54*, 8202–8205.
- (43) Chang, L.-M.; An, Y.-Y.; Li, Q.-H.; Gu, Z.-G.; Han, Y.-F.; Zhang, J. N-Heterocyclic Carbene as a Surface Platform for Assembly of Homochiral Metal—Organic Framework Thin Films in Chiral Sensing. ACS Appl. Mater. Interfaces 2020, 12, 38357—38364.
- (44) Young, A. J.; Sauer, M.; Rubio, G. M. D. M.; Sato, A.; Foelske, A.; Serpell, C. J.; Chin, J. M.; Reithofer, M. R. One-step synthesis and XPS investigations of chiral NHC-Au(0)/Au(i) nanoparticles. *Nanoscale* **2019**, *11*, 8327–8333.
- (45) Lim, I.-I. S.; Mott, D.; Engelhard, M. H.; Pan, Y.; Kamodia, S.; Luo, J.; Njoki, P. N.; Zhou, S.; Wang, L.; Zhong, C. J. Interparticle Chiral Recognition of Enantiomers: A Nanoparticle-Based Regulation Strategy. *Anal. Chem.* **2009**, *81*, 689–698.
- (46) Wang, Y.; Yu, Z.; Han, X.; Su, H.; Ji, W.; Cong, Q.; Zhao, B.; Ozaki, Y. Charge-Transfer-Induced Enantiomer Selective Discrimination of Chiral Alcohols by SERS. *J. Phys. Chem. C* **2016**, *120*, 29374–29381.
- (47) Wang, Y.; Zhao, X.; Yu, Z.; Xu, Z.; Zhao, B.; Ozaki, Y. A Chiral-Label-Free SERS Strategy for the Synchronous Chiral Discrimination and Identification of Small Aromatic Molecules. *Angew. Chem., Int. Ed.* **2020**, *59*, 19079–19086.
- (48) Gu, X.; Trujillo, M. J.; Olson, J. E.; Camden, J. P. SERS Sensors: Recent Developments and a Generalized Classification Scheme Based on the Signal Origin. *Annu. Rev. Anal. Chem.* **2018**, *11*, 147–169.
- (49) Willets, K. A.; Van Duyne, R. P. Localized Surface Plasmon Resonance Spectroscopy and Sensing. *Annu. Rev. Phys. Chem.* **2007**, 58, 267–297.
- (50) Zeng, Y.; Hu, R.; Wang, L.; Gu, D.; He, J.; Wu, S.-Y.; Ho, H.-P.; Li, X.; Qu, J.; Gao, B. Z.; Shao, Y. Recent advances in surface plasmon resonance imaging: detection speed, sensitivity, and portability. *Nanophotonics* **2017**, *6*, 1017–1030.
- (51) Naumann, S.; Schmidt, F. G.; Schowner, R.; Frey, W.; Buchmeiser, M. R. Polymerization of methyl methacrylate by latent pre-catalysts based on CO2-protected N-heterocyclic carbenes. *Polym. Chem.* **2013**, *4*, 2731–2740.
- (52) Barry, S.; Coyle, J.; Clark, T. J.; Hastie, J. J. M. Group 11 Mono-Metallic Precursor Compounds and use thereof in Metal Deposition. U.S. Patent, US9,453,036 B2 2012, pp 1–70.
- (53) Van Ausdall, B. R.; Glass, J. L.; Wiggins, K. M.; Aarif, A. M.; Louie, J. A Systematic Investigation of Factors Influencing the Decarboxylation of Imidazolium Carboxylates. *J. Org. Chem* **2009**, *74*, 7935–7942.
- (54) Zhang, L.; Yang, H.; Jiao, L. Revisiting the Radical Initiation Mechanism of the Diamine-Promoted Transition-Metal-Free Cross-Coupling Reaction. *J. Am. Chem. Soc.* **2016**, *138*, 7151–7160.
- (55) Farcau, C.; Astilean, S. Mapping the SERS Efficiency and Hot-Spots Localization on Gold Film over Nanospheres Substrates. *J. Phys. Chem. C* **2010**, *114*, 11717–11722.
- (56) Shirley, D. A. High-Resolution X-Ray Photoemission Spectrum of the Valence Bands of Gold. *Phys. Rev. B* **1972**, *5*, 4709–4714.
- (57) Hurst, E. C.; Wilson, K.; Fairlamb, I. J. S.; Chechik, V. N-Heterocyclic carbene coated metal nanoparticles. *New J. Chem.* **2009**, 33, 1837–1840.
- (58) Litorja, M.; Haynes, C. L.; Haes, A. J.; Jensen, T. R.; Van Duyne, R. P. Surface-Enhanced Raman Scattering Detected Temperature Programmed Desorption: Optical Properties, Nanostructure, and Stability of Silver Film over SiO2 Nanosphere Surfaces. *J. Phys. Chem. B* **2001**, *105*, 6907–6915.
- (59) Clavier, H.; Nolan, S. P. Percent buried volume for phosphine and N-heterocyclic carbene ligands: steric properties in organometallic chemistry. *Chem. Commun.* **2010**, *46*, 841–861.
- (60) Gómez-Suárez, A.; Nelson, D. J.; Nolan, S. P. Quantifying and understanding the steric properties of N-heterocyclic carbenes. *Chem. Commun.* **2017**, *53*, 2650–2660.

- (61) Poater, A.; Cosenza, B.; Correa, A.; Giudice, S.; Ragone, F.; Scarano, V.; Cavallo, L. SambVca: A Web Application for the Calculation of the Buried Volume of N-Heterocyclic Carbene Ligands. Eur. J. Inorg. Chem. 2009, 2009, 1759–1766.
- (62) Cao, X.; Coulter, S. K.; Ellison, M. D.; Liu, H.; Liu, J.; Hamers, R. J. Bonding of Nitrogen-Containing Organic Molecules to the Silicon(001) Surface: The Role of Aromaticity. *J. Phys. Chem. B* **2001**, 105, 3759–3768.
- (63) Moulder, J. F.; Stickle, W. F.; Sobol, P. E.; Bomben, K. D. *Handbook of X-ray Photoelectron Spectroscopy*; PerkinElmer Corporation, 1992, pp 1–261.
- (64) Bridonneau, N.; Hippolyte, L.; Mercier, D.; Portehault, D.; Desage-El Murr, M.; Marcus, P.; Fensterbank, L.; Chanéac, C.; Ribot, F. N-Heterocyclic carbene-stabilized gold nanoparticles with tunable sizes. *Dalton Trans.* **2018**, 47, 6850–6859.
- (65) Crudden, C. M.; Horton, J. H.; Narouz, M. R.; Li, Z.; Smith, C. A.; Munro, K.; Baddeley, C. J.; Larrea, C. R.; Drevniok, B.; Thanabalasingam, B.; McLean, A. B.; Zenkina, O. V.; Ebralidze, I. I.; She, Z.; Kraatz, H.-B.; Mosey, N. J.; Saunders, L. N.; Yagi, A. Simple direct formation of self-assembled N-heterocyclic carbene monolayers on gold and their application in biosensing. *Nat. Commun.* **2016**, *7*, 12654.
- (66) Mullins, R. J.; Azman, A. M. Imidazoles. Li, J. J., Gribble, G. W., Eds.; Tetrahedron Organic Chemistry Series; Elsevier, 2007; Vol. 26, Chapter 9, pp 407–433. DOI: 10.1016/s1460-1567(07)80058-4
- (67) Petrov, P. A.; Sukhikh, T. S.; Sokolov, M. N. NHC adducts of tantalum amidohalides: the first example of NHC abnormally coordinated to an early transition metal. *Dalton Trans.* **2017**, *46*, 4902–4906.
- (68) Tate, B. K.; Wyss, C. M.; Bacsa, J.; Kluge, K.; Gelbaum, L.; Sadighi, J. P. A dinuclear silver hydride and an umpolung reaction of CO2. *Chem. Sci.* **2013**, *4*, 3068–3074.